Digest Journal of Nanomaterials and Biostructures Vol. 12, No. 4, October-December 2017, p. 1239-1246

STRUCTURAL AND OPTICAL PROPERTIES OF TiO_2:MgO THIN FILMS PREPARING AT 373K

B. G. OBEID, A. S. HAMEED*, H. H. ALAARAJI
Department of Physics, College of Science, University of Kerbala, 56001 Kerbala, Iraq

Titanium dioxide - doped magnesium oxide (TiO_2:MgO) films prepared on glass substrates using a pulse laser technique (PLD) at substrate temperature 373 K with thicknesses t=400 nm . The pure TiO_2 and (TiO_2:MgO) films are investigated by X-ray diffraction and optical absorption spectroscope. The X-ray diffraction measurements show that the pure TiO2 films are a polycrystalline and contain tetragonal structure in anatase phase. The TiO2 structure has been changed to rutile phase after doped with 3% wt MgO and back to anatase phase after doped with 5 % wt MgO. TiO2 film doped with (7%, 10%) MgO have amorphous structure. The optical properties of the TiO_2:MgO show that the absorption coefficient increasing with increase the MgO concentration while, the optical band-gap decreased to be (3eV) were obtained for 10% MgO films.

(Received October 4, 2017; Accepted December 18, 2017)

Keyword: TiO_2 Thin films; MgOThin films; Pulsed laser deposition; Optical properties; Structural properties

1. Introduction

Titanium dioxide (TiO2) is an important material has been widely used in different area in science and technology[1] such as solar cell, optoelectronics , self-cleaning protective coatings ,light sensor, catalysis, piezoelectric and pyroelectric [2-8]. TiO2 growth in three crystallographic phases: rutile, anatase and brookite. Since the first two phases have a tetragonal symmetry [3,9].TiO2 become materials of high scientific interest due to their strong photocatalytic properties and stability[10]. For optoelectronics applications, anatase phase is especially adequate due to its structural properties and a higher band gap of (3.2) eV compared to the (3) eV in rutile [11]. There are different method to prepared TiO2 like chemical vapor deposition (CVD) plasma oxidation, metal organic, Pulsed laser deposition (PLD) atomic layer deposition (ALD), plasma enhanced ALD (PEALD) and sputtering [12-20].

The aim of present work is to study the structural and optical properties of ($TiO2_{1-x}$:MgO_x) thin films for x=(0, 0.03, 0.07 and 0.1) weight percentage prepared by PLD technique.

2. Experimental details

Q switched Nd:YAG laser at 1064nm (pulse width 10nsec and Pulse energy: 700 mJ) used to prepared (TiO2:MgO) thin films on glass substrate with thicknesses t=400 nm at substrate temperature 373K .TiO2 films have been prepared using TiO2 pressed powder target with kept a distance of 2cm from the glass substrate . The pulse laser deposition system has been shown in Figure (1). The structural properties of TiO_2 thin films have been described by (XRD) technique using Philips PW 1050 X- ray diffract meter. The transmittance and absorbance of TiO_2 films measured using UV-VIS-NIR spectrophotometer.

*Corresponding author: ammar.physics@yahoo.com

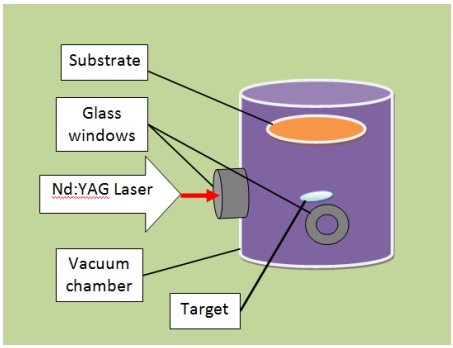

Fig. 1. Pulsed laser deposition system

3. Results and Discussion

3.1. Structural properties

The X-ray measurements of pure TiO_2 films and doped with MgO are shown in the figure(2) . From this figure we observed that the pure TiO2 film are a polycrystalline and contain tetragonal structure in anatase phase [21]. The sharp peaks of pure TiO2 thin films confirmed the crystallinity and higher purity of prepared nanoparticles [22]. The TiO2 structure has been changed to rutile phase after doped with 3% wt MgO and back to anatase phase after doped with 5 % wt MgO. The number and intensity of peaks decreased with increase the MgO concentration. TiO2 doped with (7% and 10%) MgO have an amorphous structure. Al results that calculated from x-ray diffraction are shown in table (1). These results have been showed that the greater effect of MgO contain. Since the increasing of MgO concentration lead to increase the randomness of metals.

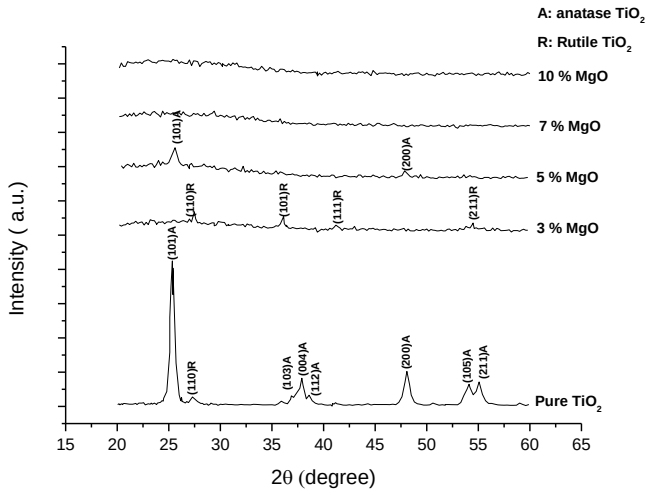

Fig. 2. XRD pattern of pure TiO2 film and doped with varied MgO concentrations

Table 1. (XRD) Parameters of TiO_2 thin films with varied MgO concentrations

Sample	2θ (Deg.)	Hkl	d_{hkl} Std.(Å)	d_{hkl} Exp.(Å)	Phase	card No.
Pure TiO_2	25.3219	(101)	3.5163	3.5144	Anatase	96-900-8214
	27.4678	(110)	3.2485	3.2446	Rutile	96-900-7532
	36.9528	(103)	2.4307	2.4306	Anatase	96-900-8214
	37.8970	(004)	2.3786	2.3722	Anatase	96-900-8214
	38.5837	(112)	2.3322	2.3316	Anatase	96-900-8214
	48.0687	(200)	1.8921	1.8913	Anatase	96-900-8214
	54.0773	(105)	1.7001	1.6945	Anatase	96-900-8214
	55.0644	(211)	1.6662	1.6664	Anatase	96-900-8214
3% MgO	27.5107	(110)	3.2485	3.2396	Rutile	96-900-7532
	36.0944	(101)	2.4876	2.4864	Rutile	96-900-7532
	41.2017	(111)	2.1875	2.1893	Rutile	96-900-7532
	54.4206	(211)	1.6876	1.6846	Rutile	96-900-7532
5% MgO	25.5365	(101)	3.5163	3.4854	Anatase	96-900-8214
	48.1026	(200)	1.8921	1.7827	Anatase	96-900-8214
7% MgO	Amorphous					
10% MgO	Amorphous					

3.2 Structure deformation

The difference planes of polycrystalline TiO2 doped MgO thin films were used for the calculation the average values of grain size and macrostrain. The grain size and macrostrain has been used to explain the structure deformation of TiO2 films sequent adding the MgO.

3.2.1 Grain size

The grain sizes for all films were calculated by using Scherrer equation [12]

$$D = \frac{0.9\lambda}{\beta \cos\Theta} \quad (1)$$

Where (D) is the average grain size, (λ) is the wavelength of the incident X-ray, (β) is the full width at half maximum of X-ray diffraction and (θ) is the Bragg's angle

The variation of the grain size for the different planes of pure and doped TiO2 thin films as a function of different MgO concentrations are shown in the table (2).

Table 2. the variation of FWHM and the grain sizes for TiO_2 with different MgO concentration

Sample	Hkl	FWHM (Deg.)	G.S (nm)
Pure TiO_2	(101)	0.4292	19.0
	(110)	0.5579	14.7
	(103)	0.6008	13.9
	(004)	0.5150	16.3
	(112)	0.4721	17.8
	(200)	0.6009	14.5
	(105)	0.7725	11.6
	(211)	0.6438	13.9
3% MgO	(110)	0.3862	21.2
	(101)	0.3005	27.8
	(111)	0.4721	18.0
	(211)	0.4292	20.8
5% MgO	(101)	0.9013	9.0
	(200)	0.7312	11.9

From this table it is seen that TiO2 thin films have a nano structure and the MgO contain play rule to change the structure and the grain size.

3.2.2 Macrostrain

The macrostrain |e| of the investigated samples was determined using Voigt method formula [23]:

$$|\mathbf{e}| = \frac{\Delta \mathbf{d}}{\mathbf{d_o}} = \mathbf{1/2\ cos\theta\ \Delta\theta} \qquad (2)$$

Where Δd is $(d\text{-}d_o)$ and (d_o) is the standard value of the inter planar spacing taken from JCPDS data file and d is experimental value of the inter planar.

The macrostrain was calculated as an average of the three diffraction planes (101), (110) and (220) that repeated for TiO2 films with different MgO contain. The calculated macrostrain of the investigated samples is given in the table (3).

Table 3. the macrostrain for the reiterated planes (101), (110) and (220) of TiO2 doped MgO films

T_a (K)	Macrostrain x 10^{-3}		
	(101)	(110)	(220)
Pure	0.540341	1.200554	0.422811
3% MgO	nonexistent	2.739726	Nonexistent
5% MgO	8.787646	nonexistent	10.25316

The reiterated planes (101), (110) and (220) used in this computation to comparative the result. From Table (3) the values of macrostrain have the difference order at different MgO contain. It is clear that the MgO concentrations are strongly affected on the macrostrain values and this is due to the difference in atomic size between TiO2 and MgO which can cause a slight lattice disruption.

4. Optical properties

The optical constants (Transmission, absorption coefficient, band gap energy, refractive index (n), extinction coefficient (k)) have been used to describe the optical behavior of the materials.

4.1. Transmission

The transmission spectra of TiO_2:MgO films at a different MgO concentration have been illustrated in figure (3) . This figure shows that the transmittance decreases with the increasing MgO concentration due to depends on the deformities propulsion, scattering centers and the incident photon energy values [24]

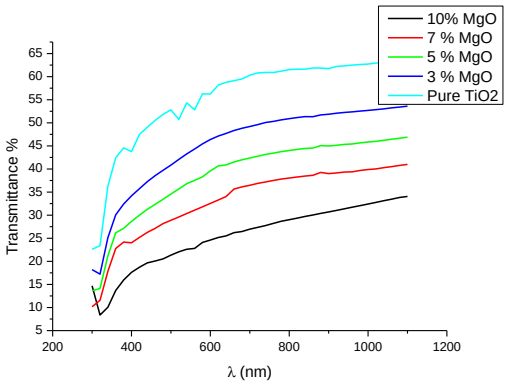

Fig. 3. Transmittance variation with the wavelength for pure TiO2 and doped films with varied MgO concentrations

4.2. Absorption coefficient

The absorbance spectrum of TiO2:MgO used to calculate the Absorption coefficient (α) by applied the following equation:

$$\boldsymbol{\alpha} = 2.303\frac{\mathbf{A}}{\mathbf{t}} \tag{3}$$

where (À) is the absorbance and (t) is film thickness

Fig. (4) declare that the increases of MgO concentration lead to increasing the absorption coefficient (α) due to the formation localized levels within the energy gap . This works is to reduce the energy gap values which leads to bias absorption edge towards longer wavelengths.

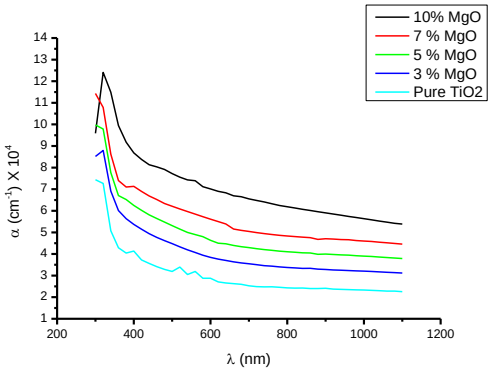

Fig. 4. The absorption coefficient variation with the wavelength for pure TiO2 and doped films with varied MgO concentrations

4.3. Energy gap

The value of energy gap can be calculated using Tauc formula [25,26]:

$$\alpha h\nu = A(h\nu - Eg)^{1/2} \quad (4)$$

where (α) is absorption coefficient , (h) is Planck's constant , (A) is constant (Eg) is energy band gap

In the figure (5) the energy gap has been obtained by drawing the relationship between $(\alpha h\nu)^2$ and photon energy incident (hν), and it is draw a tangent the straight part of the curve to cut the photon energy axis at the point $[(\alpha h\nu)^2 = 0]$. It represents the intersection point of the value of the energy gap optical allowed direct transitions and the concentration of MgO have led to the formation of new localized levels (donor levels). These levels located below the conduction pack and it is ready to receive electrons and generate tails localized energy within the optical energy gap working on the absorption of photons with low-lying energy (shifted absorption edge towards wavelengths long) which leads to decrease in value optical energy gap [27].

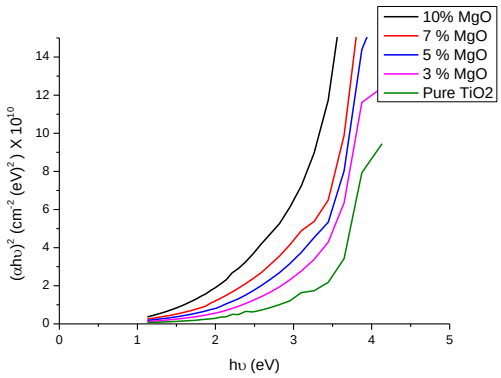

Fig. 5. $(\alpha h\upsilon)^2$ variation $(h\upsilon)$ for pure TiO2 and doped films with varied MgO concentrations

4.4. The extinction coefficient

The extinction coefficient determined using the following equation [12]:

$$k = \frac{\alpha\lambda}{4\pi} \quad (5)$$

From the Fig. (6) the extinction coefficient, in general, increase with increasing of MgO content for all films and this due rapid increases of the absorption coefficient, which indicates the occurrence of direct electronic transitions

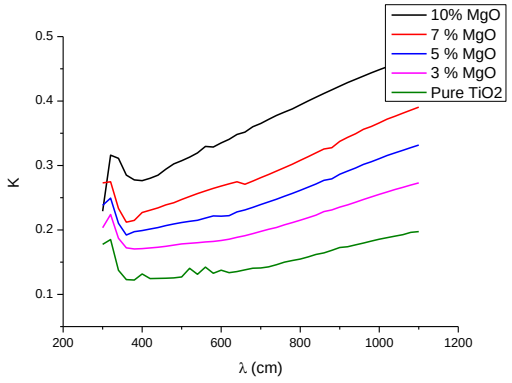

Fig. 6. The extinction coefficient as a function of wavelength for TiO_2thin films with varied MgO concentrations

4.5. The refractive index

The refractive index (n) can be calculated from the following equation [12].

$$n = \left[\frac{4R}{(R-1)^2} - k^2 \right]^{1/2} - \frac{(R+1)}{(R-1)} \tag{6}$$

The refractive index increases with increasing of concentrations doping as shown in the figure (7)

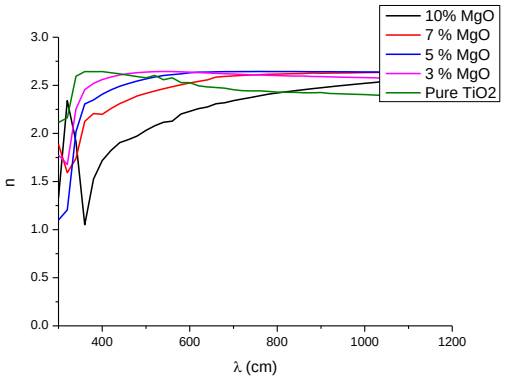

Fig. 7. The refractive index as a function of wavelength for TiO_2thin films with varied MgO concentrations

5. Conclusion

TiO_2:MgO thin films have been deposited on glass substrates using pulsed laser technique . The X ray result show that the pure TiO_2 film and the doped with 3%MgO and 5%MgO are polycrystalline while the TiO2 films doped with 7% MgO and 10% MgO are amorphous structure. The increasing of MgO content leading to increases the random metals. The optical properties of the TiO_2:MgO films were investigated the transmittance decreases with increasing of MgO concentrations doping .The energy band gap decrease with increasing of MgO concentrations doping. The refractive indexes and extinction coefficient increase with increasing of MgO concentrations doping.

Acknowledgment

A special thanks to University of Baghdad, Faculty of Science, Department of Physics, thin films laboratory for preparing the samples as well as University of kerbala , College of Science, Department of Physics for supporting this work . I am also thankful to Professor Dr. FADHIL ISMAIL SHARRAD for their help.

References

[1] Majeed A. Shaheed And Falah H. Hussein, Journal of Babylon University/Pure and Applied Sciences, **22,** (2012).
[2] R. B. Zhang, L. Gao, Key Eng. Mater, **573,** 224 (2002).
[3] Xiaobo Chen, and Samuel S. Mao Chem. Rev., **7,** (2007).
[4] B. Klingenberg, M.A. Vannice, Chem. Mater. **8**, 2755 (1996).
[5] Y. Gao, Y. Masuda, Z. Peng, T. Yonezawa, and K. Koumoto, J. Mater. Chem. **13**, 608, (2003).

[6] S.A. Sher Shah, A.R. Park, K. Zhang, J.H. Park, P.J. Yoo, ACS Appl. Mater. Interfaces **4**, 3893 (2012).
[7] P. V. Kamat, D. Meisel, Semiconductor Nanocluster-Physical, Chemical and Catalytic Aspects, Elsevier, Amsterdam, (1997).
[8] H .B. Lee, Y.M. Yoo, Y.H. Han, Scripta Mater. **55 ,** 1127 (2006).
[9] M. P. Moret, R. Zallen, D.P. Vijay, S. B. Desu, Thin Solid Films **366**, 8 (2000).
[10] S. H. Jeong, J. K. Kim, B. S. Kim, S. H. Shim, B. T. Lee, Vacuum **76**, 507 (2004).
[11] M. Zhang, G. Lin, C. Dong, L.Wen, Surf. Coat. Technol. **201,** 7252, (2007).
[12] P. E Agbo, M. N. Nnabuchi , Chalcogenide Letters **8**, 273 (2011).
[13] Seval Aksoy, Yasemin Caglar, Journal of Alloys and Compounds **613**, 330 (2014).
[14] Y. H. Lee, K.K. Chan, M. J. Brady, J. Vac. Sci. Technol. A **13**,596 (1995).
[15] T. Asanuma, T. Matsutani, C. Liu, T. Mihare, M. Kiuchi, , J. Appl. Phys. **95**, 6011 (2004).
[16] G. S. Herman, Y. Gao, T.T. Tran, J. Osterwalder, , Surf. Sci., **447**, 201 (2000).
[17] J. Aark, A. Aidla, V. Sammelselg, T. Uustare, J. Crystal Growth **18,** 259 (1997).
[18] J.J. Park, W.J. Lee, G.H. Lee, I.S. Kim, B.C. Shin, S.G. Yoon, Integrated Ferroelectrics, **65**, 81 (2004).
[19] M.P. Moret, R. Zallen, D.P. Vijay, S.B. Desu, Thin Solid Films **366**, 8, (2000).
[20] Amin Daway Thamir, Adawiya J. Haider , Ghalib A. Ali, Diyala Journal of Engineering Sciences **9**, 81 (2016).
[21] H. Lina, Abdul K. Rumaizb, M. Schulzc, D. Wanga, R. Rockd, C. P. Huanga, S. Ismat Shah, Materials Science and Engineering B **151**, 133, (2008).
[22] M. Sundrarajan, S. Gowri , Chalcogenide Letters **8**, 447 (2011).
[23] A.A.Akl, H.Howari, Journal of Physics and Chemistry of Solids **70,** 1337 (2009).
[24] Wang, LijianMeng, Vasco Teixeira, Shigeng Song, Zheng Xu, Xurong Xu, Thin Solid Films, **517,** 3721 (2009).
[25] Y. Chen, F. Wang, H. Xu, S. Ren, H. Gu, L. Wu, W. Wang, L. Feng, Chalcogenide Letters **14**, 1 (2017).
[26] P. E. Agbo, P. A. Nwofeb, L. O. Odo, Chalcogenide Letters **14,** 357 (2017).
[27] I. Soumahoro, R. Moubaah, G. Schmerber, S .Colis, M. Ait Aouaj, M. Abdlefdil, N. Hassanain, A. Berrada Dinia, Thin Solid Films **518,** 4593 (2010) .